Journal Pre-proofs

Regular paper

A Compact 4-Element Printed Planar MIMO Antenna System with Isolation Enhancement for ISM Band Operation

K. Kaboutari, V. Hosseini

PII: S1434-8411(21)00084-4
DOI: https://doi.org/10.1016/j.aeue.2021.153687
Reference: AEUE 153687

To appear in: *International Journal of Electronics and Communications*

Received Date: 22 January 2021
Accepted Date: 27 February 2021

Please cite this article as: K. Kaboutari, V. Hosseini, A Compact 4-Element Printed Planar MIMO Antenna System with Isolation Enhancement for ISM Band Operation, *International Journal of Electronics and Communications* (2021), doi: https://doi.org/10.1016/j.aeue.2021.153687

A Compact 4-Element Printed Planar MIMO Antenna System with Isolation Enhancement for ISM Band Operation*

K. Kaboutari[a], V. Hosseini[b,*]

[a] *Instituto de Telecomunicações and the Department of Electronics, Telecommunications and Informatics, University of Aveiro, P-3810-193 Aveiro, Portugal*
[b] *Faculty member of Payame Noor University, Department of Computer Engineering and Information Technology, Tehran, Iran*

Abstract

In this research, a small 4×4 printed Multiple-Input/Multiple-Output (MIMO) antenna for use in Industrial, Scientific, and Medical (ISM) systems with medical applications is presented. The proposed structure consists of four dragonfly-shaped radiators and four stepped-ground planes. In this design, adjacent elements are placed perpendicular to each other to create the necessary isolation between them. Also, a novel decoupling-element is utilized between the radiating-elements as an innovation for enhancing the isolation. A pair of rectangular-shaped slits on either side of the dragonfly-shaped radiation patch is employed for determining the frequency band of the antennas. Laboratory results show that the proposed MIMO antenna can cover the frequency band of 2.16 GHz to 3.2 GHz with isolation above 21.4 dB. Small dimensions of $0.63\lambda \times 0.63\lambda$ mm^2 and presentation of diversity performance with an Envelope Correlation Coefficient (ECC) of less than 0.001 for aligned elements and 0.00043 for orthogonal elements are other particular advantages of the proposed antenna.

Keywords: MIMO antennas, ISM band, Monopole antenna, Medical application of antennas

*This paper is a collaborative effort.

*Corresponding author
Email address: v.hosseini@pnu.ac.ir (V. Hosseini)

1. Introduction

Printed antennas have always been one of the most popular design areas for researchers. These antennas have attractive features such as wide impedance bandwidth, simple construction, easy integration with other microwave components, and a convenient radiation pattern [1]. Various forms of the printed antenna, including designs of array antennas for radar applications [2] and high-gain directional antennas for satellite utilization [3], have been recently presented. On the other hand, one of the attractive fields in the Multiple-Input/Multiple-Output (MIMO) system's design is printed antennas. It allows the elements of a MIMO system to be aligned closer together in the space. Among the salient features of a MIMO antenna, the most significant features that come to mind are increasing radio channel capacity, according to Shannon's law, and overcoming the phenomenon of Multipath Fading [4]. Recently, various MIMO antennas with diverse design techniques have been presented [5, 6, 7, 8, 9, 10, 11]. A 4×4 MIMO antenna is designed and provided for use in wearable biotelemetric devices in [5]. This patch antenna is composed of four elements placed orthogonally to each other. The antenna has an impedance bandwidth of 1.6 GHz to 3.8 GHz and provides isolation above 25.3 dB between the radiating elements. The maximum gain and Envelope Correlation Coefficient (ECC) of the antenna are 2.36 dB and below 0.23, respectively. In addition, a 4-element MIMO system using two types of slot and patch antennas for application of Wireless Local Area Network (WLAN) in 2.4 GHz frequency band is introduced in [6]. In this design, the necessary isolation is achieved by printing two different species of antennas on both sides of the substrate. All four elements have a same radiation behavior as the other elements. This antenna has a frequency bandwidth, isolation, and ECC of 2.4 GHz to 2.5 GHz, above 25 dB, and below 0.022, respectively. Other structures of MIMO antennas such as including MIMO antenna with monopole elements for LTE 2300 and 2.45 GHz ISM applications in [7], 4-element MIMO antenna for use in 2.45 GHz ISM band using Complementary Split-Ring Resonator (CSRR) elements in [8],

using ground slots for 4G LTE and 3G applications to increase isolation between Planar Inverted-F Antenna (PIFA) elements in MIMO antenna in [9] and [10], using of Cylindrical Monopole elements and improving isolation by using Defected Ground Structures (DGS) for application in the frequency band 0.698 GHz to 0.960 GHz in [11], and a new design of a 4-element MIMO antenna for X-band applications can be noticed in [12]. In [12], a circular polarization (CP) operation is attained by using Tai Chi-shaped patches and L-shaped feeds. This MIMO antenna has two resonant frequencies at around 7.75 GHz and 10.15 GHz frequency.

In this study, a 4-element MIMO antenna consisting of a dragonfly-shaped monopole radiator and a stepped-ground plane is introduced and investigated. The adjacent elements are located perpendicularly to each other, and the cross-coupling between the antennas is reduced using a decoupling-component. Unlike using a cross-shaped microstrip-line between the radiation patches to improve isolation in the conventional MIMO antennas, this design uses an innovative technique to enhance the isolation. In this design, placing a circular stub in the center of the traditional cross-shaped microstrip-line leads to preferable isolation. It means the induced currents in the cross arms focus on the circular stub environment and cause forming rotational currents. This event leads to dissipate the induced currents and enhance the isolation between the antenna radiation elements. Besides, the designed antenna has low-profile, low-cost, and compact features and has one of the best isolation and bandwidth characteristics, according to Table 1. It should be noted that the proposed MIMO antenna has the best ECC value in the above table. The introduced MIMO antenna covers the 2.45 GHz ISM frequency band with isolation above 21.4 dB, and it has compact dimensions and is suitable for medical applications.

2. Design Details of the Single Antenna

A single antenna is designed to cover the 2.45 GHz ISM band in the first step of the antenna design. This antenna consists of an FR4 substrate with a per-

mittivity coefficient, loss tangent, and dimensions of 4.4, 0.02 and, 35×30×1.6 mm^3, respectively. A microstrip feed line with a width of 2.9 mm and a length of 22.9 mm has been used to generate the necessary impedance matching at the antenna's ports. The single antenna is designed at two stages. Figure 1 shows the physical dimensions and design steps of the single antenna. At the first stage of design, the single antenna consists of a microstrip feed line and two identical elliptical patches, which the elliptical patches are connected to the top of the feed line and located perpendicular to each other at a 45-degree angle. The use of step-shaped ground also produces new capacitances between the ground and the radiation patch, which improves the impedance matching and bandwidth of the antenna. At the second stage of design, on both sides of the microstrip line connected to the radiation patch, two rectangular slits with dimensions $L_s \times W_s$ are placed to control the frequency band.

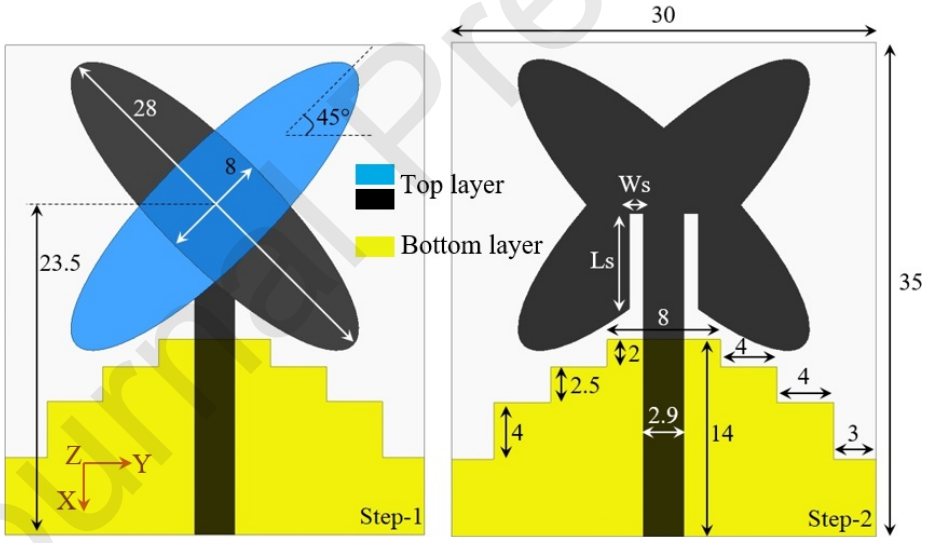

Figure 1: Structure of the proposed single antenna at the first and second stages of design.

Figure 2 shows the simulation results of the antenna impedance bandwidth in step-1 and -2. According to the figure, the single antenna covers 2.71 GHz to 4.36 GHz frequency band with a weak resonance at the first stage of the design. At the second phase of design, the antenna frequency band has become

wider, and the antenna has achieved a strong resonance at 2.45 GHz by adding two rectangular slits on either side of the microstrip feed line at the junction place with the radiation patch. The simulation results confirm proposed single antenna has a frequency bandwidth from 1.75 GHz to 3.12 GHz and can cover 2.45 GHz ISM frequency band with $S_{11} < -10\ dB$. From 2.14 GHz to 2.76 GHz frequency band coverage with $S_{11} < -15\ dB$ is a significant feature for the proposed single antenna that supports 2.45 GHz ISM systems. The radiation patch slits and created steps on the ground plane play an effective role in expanding the frequency band of the antenna.

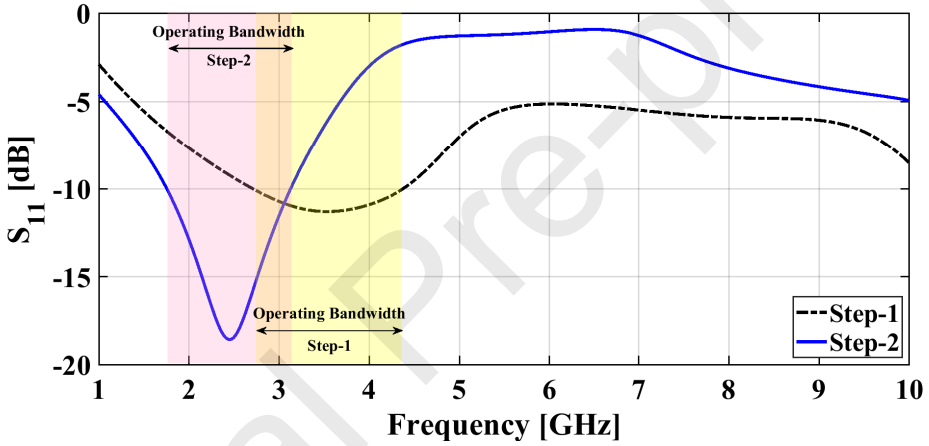

Figure 2: The single antenna's return-loss results at the first and second (proposed) stages of design.

The length of the slits next to the radiation patch, L_s, is one of the important parameters of the single antenna design. Figure 3 displays the results of the parametric analysis on this length. The location of the resonance frequency band, according to the curves, is a function of the slits' length. By increasing the length of these slits from 4.7 mm to 8.7 mm, the antenna resonance frequency shifts from 3 GHz to 2.1 GHz. In this design, the length of the L_s slit is set to 6.7 mm to achieve 2.45 GHz resonance frequency ($L_s = 6.7\ mm^*$).

As the W_s width increases from 0.5 mm to 4 mm, the antenna resonance frequency decreases from 2.68 GHz to 1.98 GHz (Figure 4). It should be

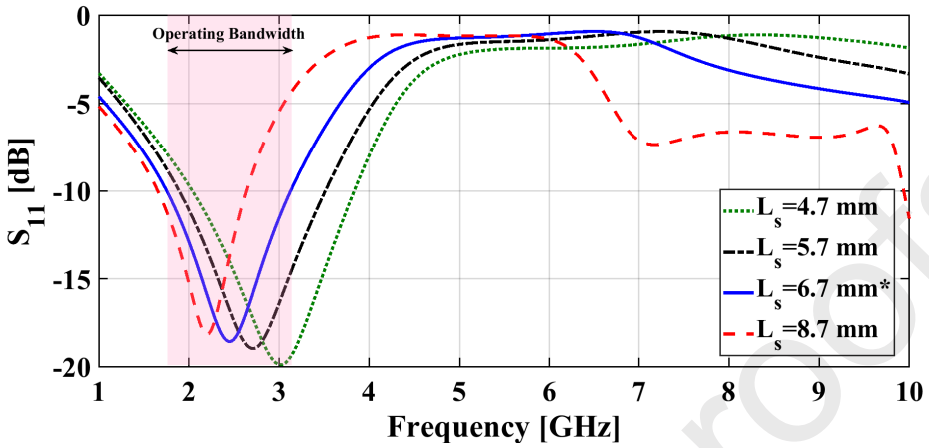

Figure 3: Simulation results of the parametric analysis on the slits length, L_s, of the proposed single antenna.

noted that the resonance frequency is exactly located at 2.45 GHz by selecting $W_s = 1\ mm^*$. By increasing W_s, also, the antenna bandwidth decreases from 1.66 GHz to 800 MHz.

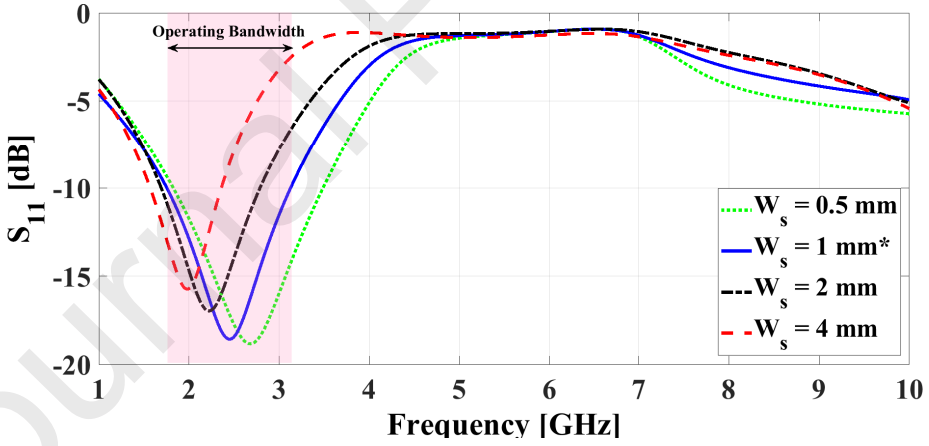

Figure 4: Simulation results of the parametric analysis on the slits width, W_s, of the proposed single antenna.

The process of parametric analysis has been performed on other dimensions of the antenna, and their optimal values have been selected.

Figure 5 manifests the simulated gain and impedance bandwidth of the single

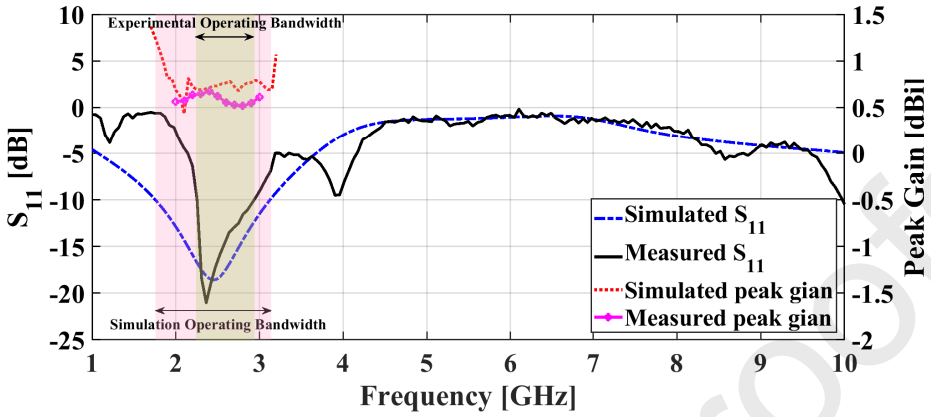

Figure 5: The simulated and measured S_{11} and peak gain of the proposed single antenna.

antenna. According to this diagram, a single antenna has an average simulated and measured gain of 0.80 and 0.59 dB in the frequency band, respectively. Also, in Figure 6, the radiation pattern of the proposed antenna is shown in two planes, E-plane and H-plane, as Co-pol and Cross-pol at 2.45 GHz frequency. According to the radiation patterns, for the proposed antenna, we observe a stable radiation pattern with a low cross-section. However, the radiation pattern on the H-plane and E-plane are omnidirectional and acts as a dipole antenna, respectively.

3. Details and Results of the Designed MIMO Antenna

The design of a MIMO antenna to cover 2.45 GHz ISM frequency band is the main purpose of this paper. In the progress of the design, hence, the initial structure of the proposed MIMO antenna is created by placing the single antennas one by one orthogonally together. Figure 7 exhibits the initial configuration of the proposed MIMO antenna (simple mode). According to the figure, the MIMO antenna consists of four separate ports. Each port of the antenna consists of a microstrip feed line and a dragonfly-shaped radiator with a stepped ground plane. To create the essential isolation between the radiation elements, the center of each antenna is 24 mm away from its adjacent antenna.

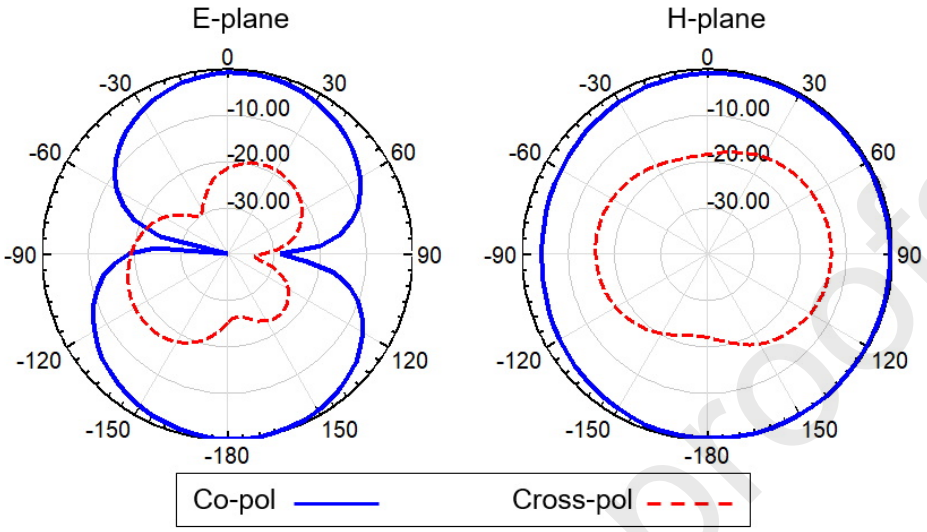

Figure 6: The simulated radiation pattern of the proposed single antenna at 2.45 GHz frequency.

In this structure, similar to the previous one, an FR4 substrate with a thickness of 1.6 mm and dimensions of $0.63\lambda \times 0.63\lambda$ mm^2 is used (λ is the free-space wavelength at the center of the frequency band). Placing adjacent radiation elements orthogonally next to each other can guarantee its diversity performance. Also, orthogonalizing of the radiation elements is one of the best ways to reduce mutual-coupling between them. Furthermore, a decoupling-element has been employed in the structure of the MIMO antenna to enhance the isolation between the elements of the proposed antenna (Figure 7(b)).

Figure 8 shows the results of the return-loss response of the proposed MIMO antenna. According to the simulation results, the proposed MIMO antenna covers from 1.65 GHz to 3.15 GHz frequency band with $S_{11} < -10$ dB. From 2.02 GHz to 3.03 GHz frequency band coverage with $S_{11} < -15$ dB is a significant feature for the proposed antenna that supports 2.45 GHz ISM systems. At lower frequencies (f_L), the interaction of the antenna ports with its other components such as feed lines, and radiation and parasitic patches increases in the experimental studies. This event generates some discrepancies of the mea-

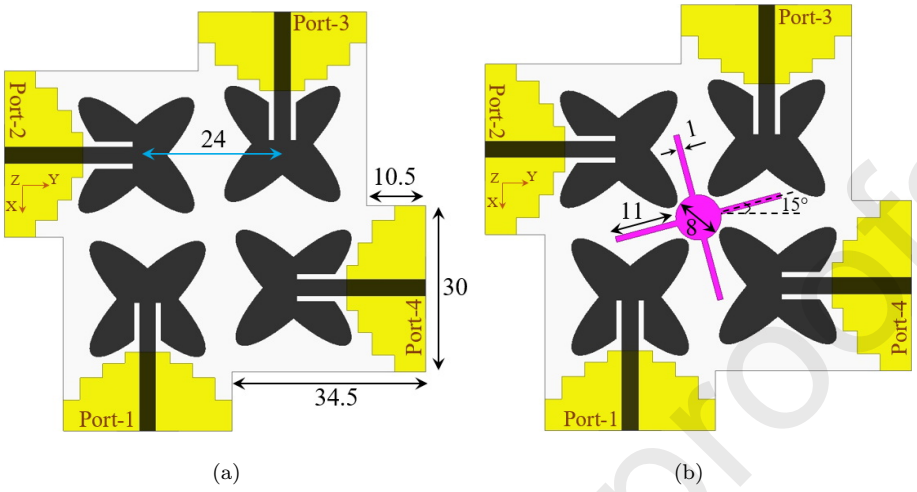

(a) (b)

Figure 7: The MIMO antenna configuration. (a) Initial/Simple configuration. (b) Proposed configuration.

sured results with the simulated studies of the S_{nn} at lower frequencies. Due to the similarity of the antennas and their symmetrical placement, the proposed MIMO antenna structure is symmetrical, and therefore, the frequency response of the antennas' ports are similar. Existence of a single resonance is another prominent feature for the proposed antenna. Unlike many ISM antennas, the antenna has no resonance other than the main one in a wide range of frequency. Consequently, due to the application type, a single resonance frequency inhibits the frequency interference phenomenon occurrence with other Ultra-Wideband (UWB) wireless systems [13].

Figure 9 shows the isolation results of the proposed MIMO antenna. Regarding the structure of the MIMO antenna, two types of mutual couplings can be defined for the orthogonal radiation elements (S_{12}, S_{23}, S_{34}, S_{14}) and aligned radiation elements (S_{13}, S_{24}) of the MIMO antenna. According to the isolation results in Figure 9, it can be seen that the isolations for orthogonal elements are similar in the working frequency band of the antenna. Moreover, isolations for the parallel elements are also alike.

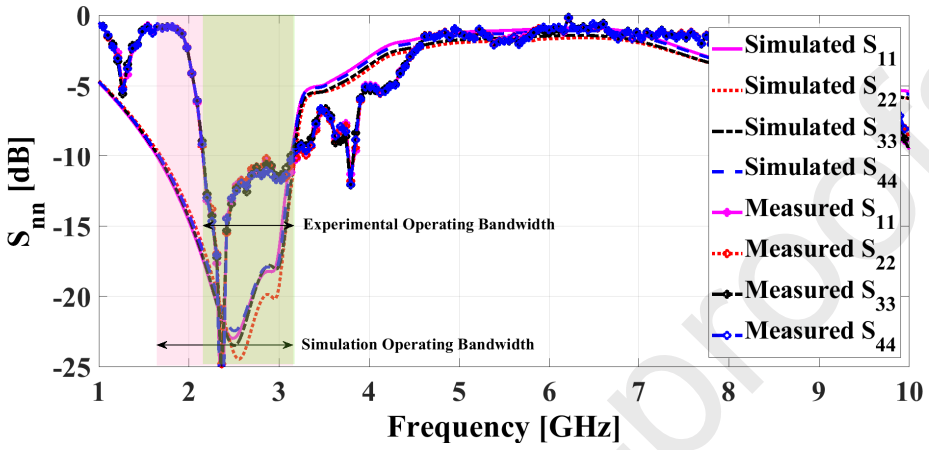

Figure 8: The simulated and measured S_{nn} of the proposed MIMO antenna.

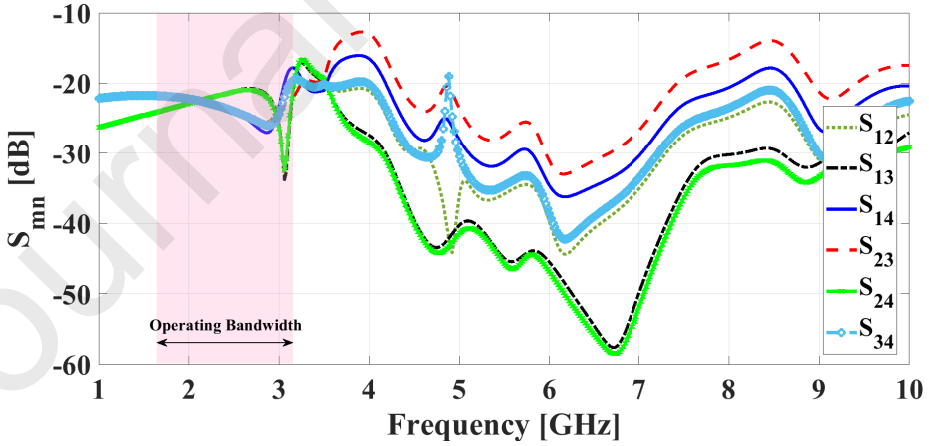

Figure 9: The simulation isolation results related to the proposed MIMO antenna.

The proposed MIMO antenna isolation diagrams in two modes with/without decoupling elements are shown in Figure 10. Regarding the figure, it can be seen that inserting a decoupling-element to the structure of the MIMO antenna has increased its isolation by an average of 4 dB. Due to the structural symmetry of the antenna, one of the isolation states related to orthogonal elements (S_{12}) and one of the isolation states related to aligned elements (S_{13}) are presented. In this figure, the results of the MIMO antenna without the decoupling-element are named: Simple, and the results of the proposed MIMO antenna are called: Proposed.

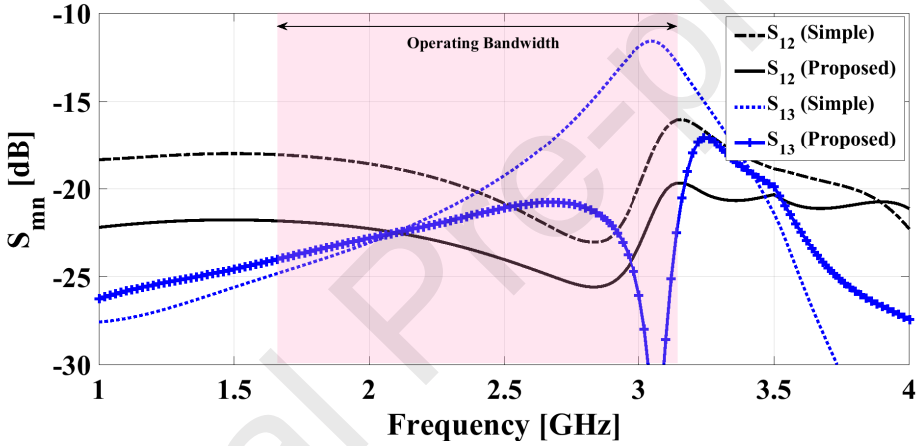

Figure 10: Comparison of the simulation isolation results related to the MIMO antenna with/without decoupling-element.

To understand the performance of the decoupling-element in the proposed MIMO antenna structure, surface currents of the MIMO antenna are presented with/without the decoupling-element in Figure 11. It can be seen that by exciting the port-1 of the MIMO antenna, the radiation patches related to the second, third, and fourth elements are also stimulated in the case without decoupling-element. The presence of the decoupling-element between the antennas, however, prevents them from having a strong impact over other ports. Thus, the decoupling-element itself becomes the target of induction fields related to the port-1 of the antenna.

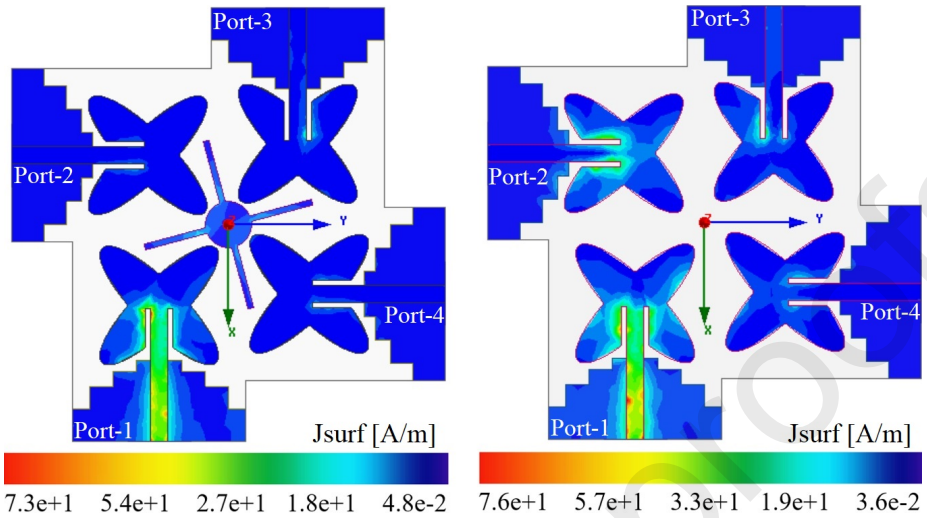

Figure 11: Comparison of the surface current of the proposed MIMO antenna with/without decoupling-element.

In figure 12, the induced currents in the cross arms focus on the circular stub environment and cause forming rotational currents. Consequently, this phenomenon leads to dissipate the induced currents and enhance the isolation between the antenna radiation patches.

Another criterion for displaying the isolation of a MIMO system is the ECC parameter. Indeed, this parameter indicates the success rate of a MIMO system. The elements' independence in their performance is determined by ECC. The ECC of the MIMO antenna systems should be near to zero value. But, MIMO antenna systems with an ECC less than 0.5 are considered acceptable [14]. From the S-parameter using Equation (1), the ECC can be evaluated [15]. Figure 13 shows the ECC for orthogonal and paralleled elements. According to this figure, the ECC values for the MIMO antenna are less than 0.001 and 0.00043 for the aligned and perpendicular cases, respectively.

$$ECC = \rho_{ij} = \frac{|S_{ii}^{*}S_{ij} + S_{ji}^{*}S_{jj}|^{2}}{(1-(|S_{ii}|^{2}+|S_{ij}|^{2}))(1-(|S_{jj}|^{2}+|S_{ij}|^{2}))} \quad (1)$$

In Figure 14, ECC for orthogonal and aligned elements are plotted with/without

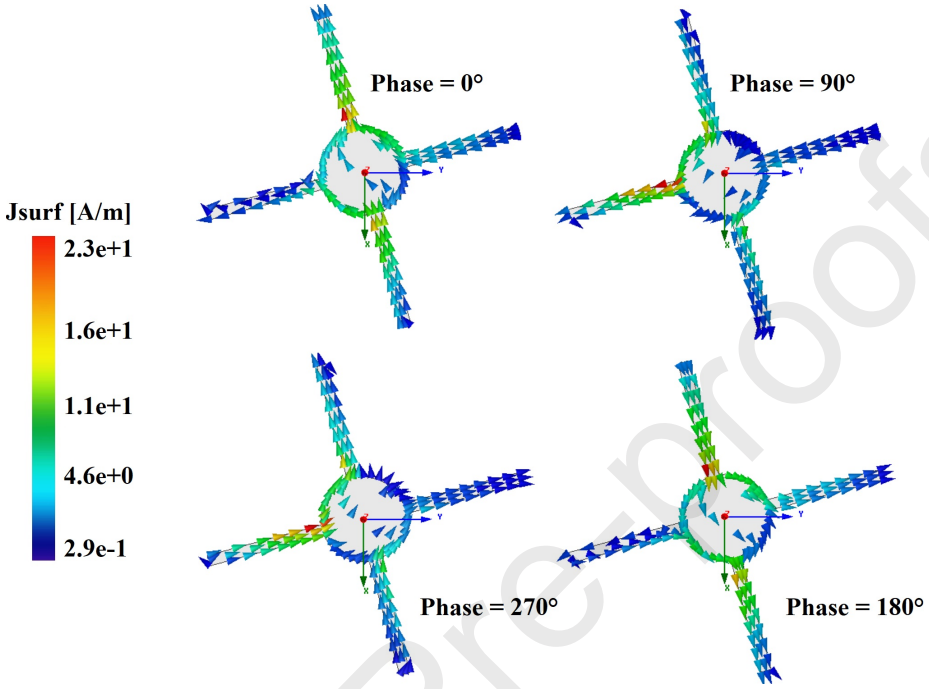

Figure 12: The distribution of surface currents on the cross arms and their accumulation on the circular stub at 2.45 GHz frequency.

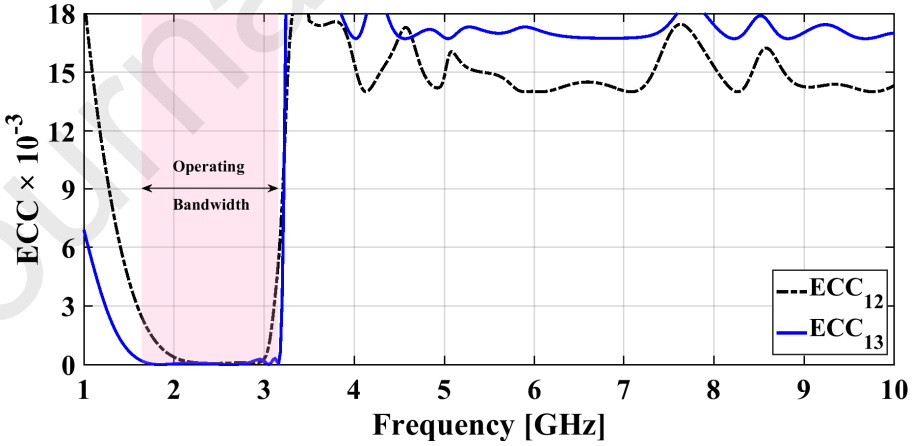

Figure 13: The Simulated ECC for the orthogonal and aligned elements.

decoupage-elements. By adding a decoupling-element to the proposed MIMO antenna structure, a decrease of about 0.001 ECC value can be seen.

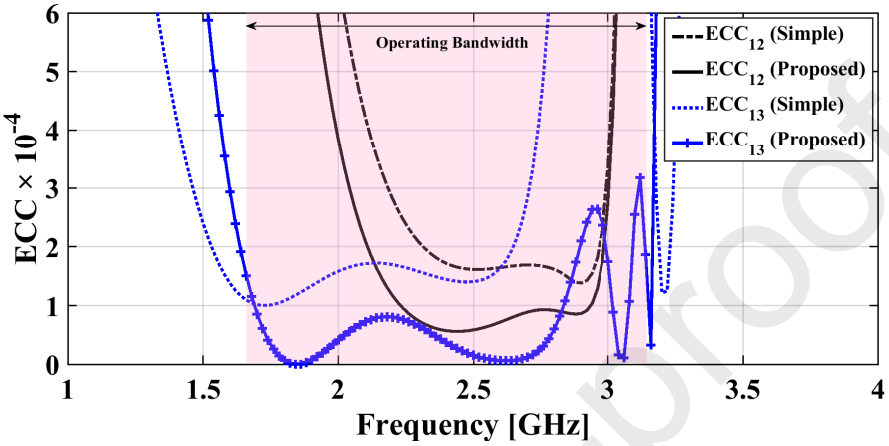

Figure 14: The ECC for the orthogonal and aligned elements with/without decoupling-element.

Figure 15 shows the proposed three-dimensional radiation patterns of the MIMO antenna by excitation of port-1 to -4 at the frequency of 2.45 GHz. It can be seen that the radiation pattern of the proposed MIMO antenna is inclined towards the $-y$, $-x$, $+y$, and $+x$-axes by exciting port-1, -2, -3, and -4, respectively. The deflection of the radiation pattern of each port towards one of the coordinate axes is occurred due to the presence of radiation elements of other ports around it and the similar function of their reflector. This issue has led to the diversity feature of the radiation pattern in the proposed MIMO antenna. In this way, radiation of the antenna elements occurs in different directions in the proposed MIMO antenna, and this issue minimizes the effect of mutual coupling between the MIMO antenna elements (Figure 15).

Figure 16 displays the E-plane and H-plane of the proposed MIMO antenna radiation patterns as co-pol and cross-pol on port-1 to -4 at 2.45 GHz frequency. The proposed MIMO antenna has a stable radiation pattern with at least 10 dB cross-pol discrimination over all ports. The radiation pattern of the antenna in the H-plane is almost omnidirectional. However, the radiation pattern of the

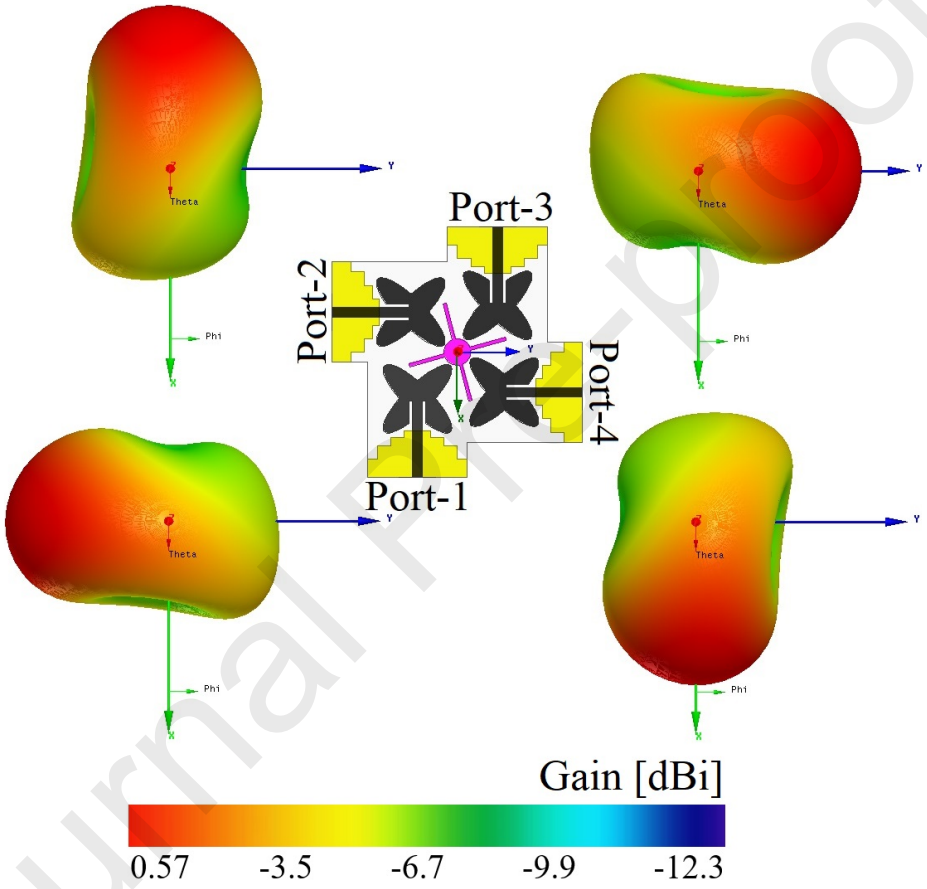

Figure 15: Three-dimensional radiation patterns of the recommended MIMO antenna at port-1 to -4 at 2.45 GHz frequency.

antenna acts similar to the dipole antennas in the E-plane. The inclination of the radiation pattern in each port towards one of the coordinate axes, displayed in the three-dimensional pattern, can also be seen in H-plane radiation patterns. It should be noted the simulations are performed using 64-bit HFSS Version 15.

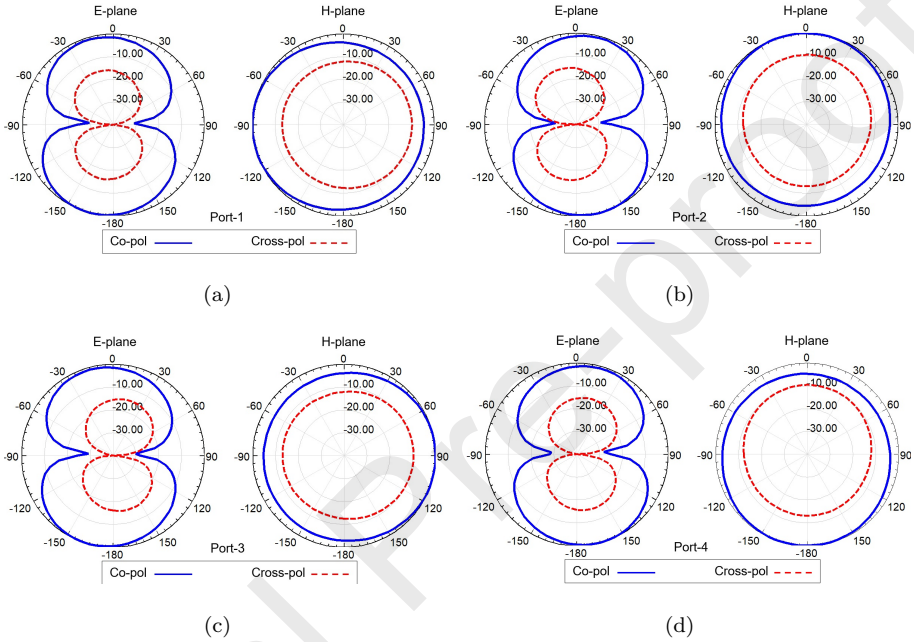

Figure 16: Recommended E-plane and H-plane radiation patterns of the proposed MIMO antenna at: (a) port-1, (b) port-2, (c) port-3, and (d) port-4 at 2.45 GHz frequency.

After extracting the optimized physical parameters for the proposed MIMO antenna, it was made using printing technology on fiber printed circuit board and tested in the antenna and microwave laboratory of Urmia University by Agilent E8363C Vector Network Analyzer (VNA). Figure 17 shows a photo of a prototype of the antenna made during the testing process. Due to the application type of the designed antennas in medical systems, saving space for designed antennas is very important. Therefore, 25.76% has been added to the usable area of the system by making clips around the edges of the MIMO antenna's substrate (Figures 17(c) and 17(d)).

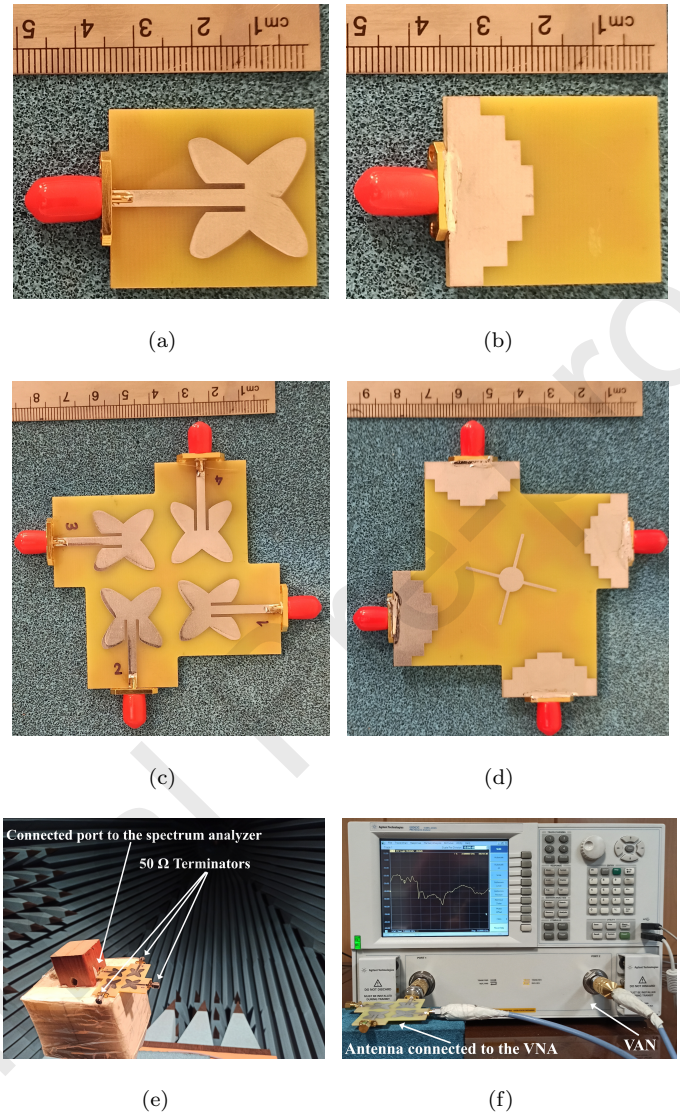

Figure 17: Prototype photo of the proposed single-element and MIMO antennas. (a) Front side of the recommended single-element antenna. (b) Back side of the recommended single-element antenna. (c) Front side of the recommended MIMO antenna. (d) Back side of the recommended MIMO antenna. (e) Recommended MIMO antenna in the anti-reflection/anechoic chamber. (f) Recommended MIMO antenna connected to the VNA.

Figure 9 exhibits a comparison of the simulation and test results related to the return-loss from port-1 to -4 of the proposed MIMO antennas. The experimental results reveal that the proposed MIMO antenna on its ports from 1 to 4 provides impedance bandwidth from 2.16 to 3.20, 2.16 to 3.20, 2.16 to 3.13, and 2.16 to 3.16, respectively. In this way, the proposed antenna can properly cover 2.45 GHz ISM frequency band.

Also, isolation between the orthogonal and aligned elements of the proposed MIMO antenna is shown in both test and simulation states in Figure 18. Due to the symmetry of the recommended MIMO antenna configuration, other isolations' are not presented. It can be seen that the proposed MIMO antenna isolations are more than 20.7 dB and 21.4 dB along with the antenna frequency band for simulation and experimental studies, respectively.

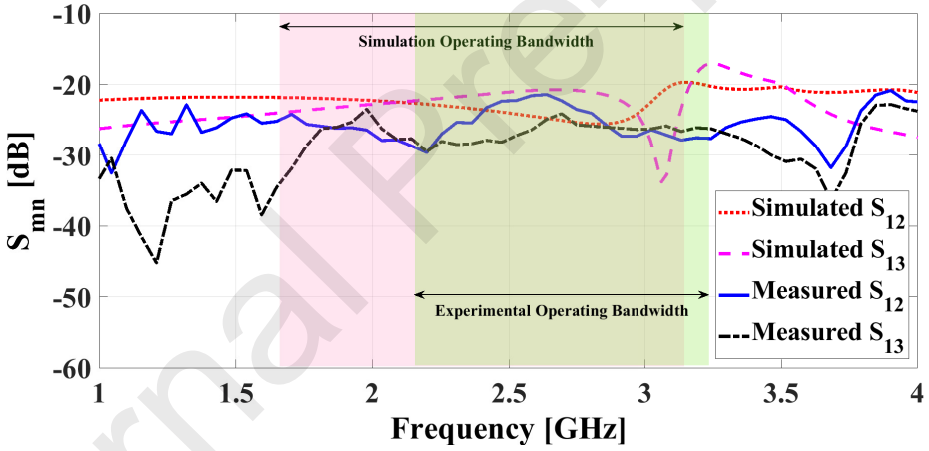

Figure 18: The simulation and experimental isolation results of the orthogonal and aligned elements of the proposed MIMO antenna.

Figure 19 displays the simulated and tested E-plane and H-plane radiation patterns of the proposed MIMO antennas on two ZY- and ZX-planes. Due to the structural symmetry and the similarity of radiation performance of the proposed MIMO antenna in port-1 to -4, just port-1 of the proposed MIMO antenna have been tested for the pattern. According to the laboratory results, the radiation pattern of the antenna is stable, and a difference of more than 10

dB between the radiation pattern of Co-pol and Cross-pol is observed at the frequency of 2.45 GHz. There is also a slight difference between the experimental and simulation results, which may be related to human error during the antenna test, and errors related to the manufacturing process of the antenna.

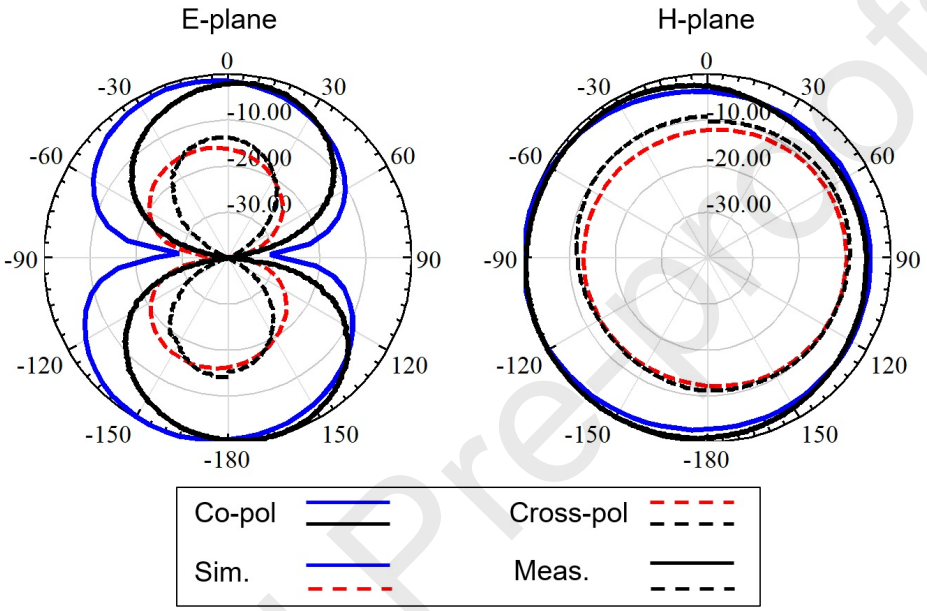

Figure 19: The simulation and experimental E-plane and H-plane radiation patterns in port-1 of the MIMO antenna at 2.45 GHz frequency.

Figure 20 manifests the simulation and experimental gain of the proposed MIMO antenna at port-1. Accordingly, the proposed MIMO antenna has a maximum gain of 0.68 dB at 2.4 GHz. However, studies have shown that the antenna gain at frequencies above 3.5 GHz has a decreasing trend.

Figure 21 displays the experimental and simulation ECC of the proposed MIMO antenna at the desired frequency range for orthogonal and aligned elements. Laboratory results indicate that the ECC values of the proposed antenna for orthogonal and aligned elements are less than 0.001 and 0.00043, respectively. This value is very suitable for ECC at MIMO antennas.

According to the results in Figure 22, the proposed MIMO antenna is proper for medical applications at 2.45 GHz ISM frequency band. Indeed, for determin-

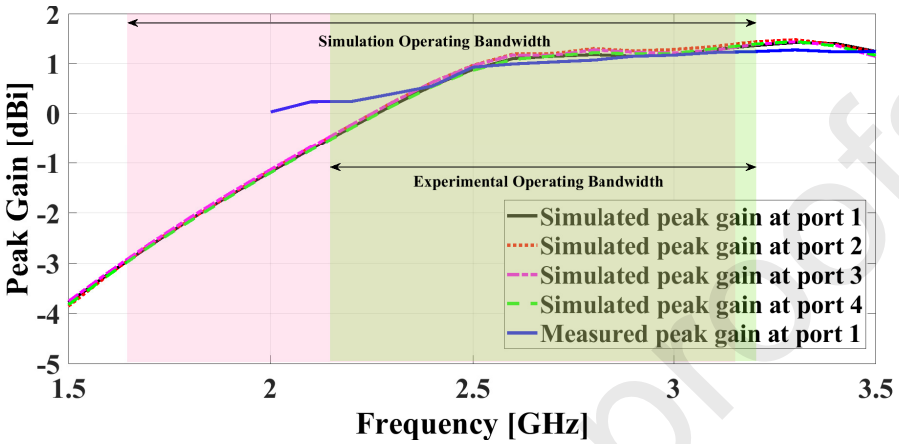

Figure 20: The simulation and experimental peak gain of the proposed MIMO antenna by excitation of port-1 for experimental studies.

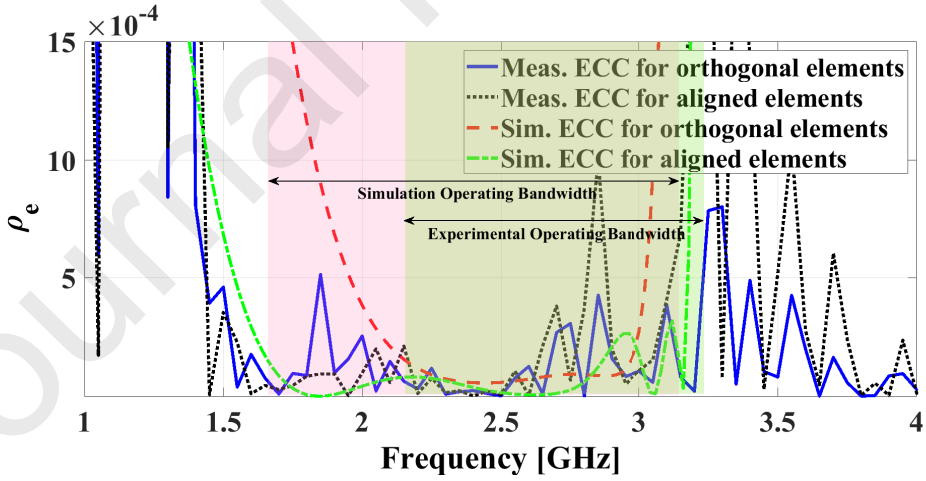

Figure 21: The simulation and Experimental ECC of the proposed MIMO antenna at orthogonal elements (port-1 and -2) and aligned elements (port-1 and -3).

ing patients' status using the proposed MIMO antenna, each radiation pattern covers one of the patients resting rooms in a hospital to monitor the wireless medical appliances. The implanted wireless medical appliances inside the patients' bodies or wireless medical instruments connected to the other monitoring devices transmit/receive data using the proposed MIMO antenna in the hospital environment.

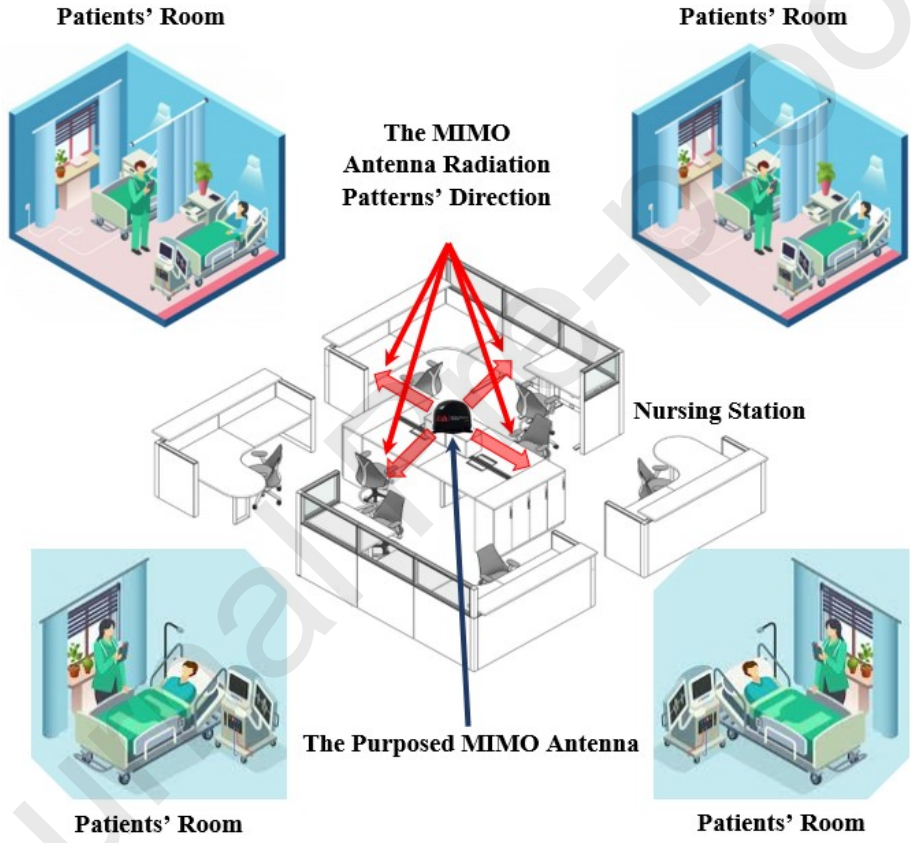

Figure 22: Medical application of the designed MIMO antenna.

To show the advantages of the proposed design, finally, the results of the introduced antenna are compared with several other MIMO antennas that have 4-element in Table 1. According to the table, the proposed MIMO antenna covers a large bandwidth by occupying a smaller space. In comparison with other antennas in the table, however, the proposed antenna has one of the

best isolation values. According to the results of the proposed antenna, this structure has comparable and mostly higher performance in contrast to the designs presented in the table.

Ref.	Size (λ_0^2)	Operating Band [GHz]	Isolation [dB]	Peak Gain [dBi]	ECC	Antenna Type
[4]	$\pi \times 0.8^2$	2.2-2.72	> 15	8.37	< 0.01	Dipole
[5]	0.67×0.67	1.6-3.8	> 25.3	2.36	< 0.23	Patch
[6]	0.64×0.48	2.4-2.5	> 25	2.84	< 0.022	Slot + Patch
[7]	0.25×0.13	2.19-2.54	> 15	1.26	< 0.01	Monopole
[8]	0.82×0.41	2.45-2.475	> 10	-0.8	< 0.1	CSRR + Patch
[9]	0.69×0.41	2.07-2.21	> 15	4.32	< 0.3825	PIFA
[10]	0.67×0.40	2.017-2.265	> 10	3.5	< 0.1889	Monopole
[11]	$\pi \times 0.19^2$	0.698-0.960	> 10	< 2	< 0.075	Cylindrical Monopole
[12]	3×3	7.58–8.04 9.23–10.79	> 20	2.5	< 0.003 † < 0.005 ‡	*Microstrip* + *Patch*
This work	0.63×0.63	2.16-3.20	> 21.4	< 1.28	< 0.0004 † < 0.001 ‡	Monopole

Table 1: Results' comparison of the introduced antenna with several other MIMO antennas that have four elements (ECC for orthogonal elements (†) and aligned elements (‡) of the proposed MIMO antenna, respectively).

4. Conclusion

In this research, a 4-element MIMO antenna is introduced with medical system applications at 2.45 GHz ISM frequency band. The proposed MIMO antenna consists of four dragonfly-shaped radiation elements and a stepped ground plane, which is fed using the microstrip method. Also, to generate necessary isolation between the antenna ports, the adjacent elements are placed orthogonally. An innovative decoupling-element between the radiation elements is responsible for upgrading the antenna isolation. Other important features of the proposed antenna are its low-profile, low-cost, small size, single resonance in a wide frequency range, lack of frequency interference with UWB systems, and stable radiation behavior. Laboratory results show that the proposed MIMO antenna can cover 2.45 GHz ISM frequency band with $S_{11} < -15\ dB$. This antenna can be considered as a suitable candidate for medical system applications in 2.45 GHz ISM frequency band.

Acknowledgement

The authors of this article express their gratitude to Payame Noor University for its comprehensive support. Besides, the authors would like to appreciate the Northwest Antenna and Microwave Research Laboratory (NAMRL) at Urmia University for technical supports. Also, we would like to express our deep thanks to our dear friend Dr. Majid Shokri, who blessed us with their priceless and unforgettable supports throughout all our studies.

References

[1] M. Shokri, H. Shirzad, S. Movagharnia, B. Virdee, Z. Amiri, S. Asiaban, Planar monopole antenna with dual interference suppression functionality, IEEE Antennas and Wireless Propagation Letters vol. 12, (2013) pp. 1554–1557.

[2] K. Kaboutari, A. Zabihi, B. Virdee, M. Salmasi, Microstrip patch antenna array with cosecant-squared radiation pattern profile, AEU - International Journal of Electronics and Communications vol. 106, (2019) pp. 82–88.

[3] A. Siahcheshm, J. Nourinia, C. Ghobadi, M. Shokri, Circularly polarized printed helix antenna for l- and s-bands applications, Radioengineering vol. 29, (2020) pp. 67–73.

[4] R. Nasirzade, J. Nourinia, C. Ghobadi, M. Shokri, R. Naderali, Broadband printed mimo dipole antenna for 2.4 ghz wlan applications, Journal of Instrumentation vol. 15,.

[5] A. Iqbal, A. Smida, A. Alazemi, M. Waly, N. Mallat, S. Kim, Wideband circularly polarized mimo antenna for high data wearable biotelemetric devices, IEEE Access vol. 8, (2020) pp. 17935–17944.

[6] H. Li, J. Xiong, S. He, A compact planar mimo antenna system of four elements with similar radiation characteristics and isolation structure, IEEE Antennas and Wireless Propagation Letters vol. 8, (2009) pp. 1107–1110.

[7] L. Yang, S. Yan, T. Li, Compact printed four-element mimo antenna system for lte/ism operations, Progress In Electromagnetics Research Letters vol. 54, (2015) pp. 47–53.

[8] M. Sharawi, M. Khan, A. Numan, D. Aloi, A csrr loaded mimo antenna system for ism band operation, IEEE Transactions on Antennas and Propagation vol. 61, (2013) pp. 4265–4274.

[9] M. Ikram, R. Hussain, A. Ghalib, M. Sharawi, Compact 4-element mimo antenna with isolation enhancement for 4g lte terminals, 2016 IEEE International Symposium on Antennas and Propagation (APSURSI).

[10] M. Ikram, R. Hussain, O. Hammi, M. Sharawi, An l-shaped 4-element monopole mimo antenna system with enhanced isolation for mobile applications, Microwave and Optical Technology Letters vol. 58, (2016) pp. 2587–2591.

[11] Y. Chen, C. Chang, Design of a four-element multiple-input–multiple-output antenna for compact long-term evolution small-cell base stations, IET Microwaves, Antennas and Propagation vol. 10, (2016) pp. 385–392.

[12] A. Eslami, J. Nourinia, C. Ghobadi, M. Shokri, Four-element mimo antenna for x-band applications, International Journal of Microwave and Wireless Technologies (2021) pp. 1–8.

[13] M. Shokri, V. Rafii, S. Karamzadeh, Z. Amiri, B. Virdee, Cpw-fed printed uwb antenna with open-loop inverted triangular-shaped slot for wlan band filtering, International Journal of Microwave and Wireless Technologies vol. 8, (2015) pp. 257–262.

[14] A. Fatima, S. Rashid, S. Tayyab, R. S. Muhammad, B. Muhammad, S. Farhan, A compact quad-element uwb-mimo antenna system with parasitic decoupling mechanism, Applied Sciences 9 (11).

[15] F. Bahmanzadeh, F. Mohajeri, Simulation and fabrication of a high-isolation very compact mimo antenna for ultra-wide band applications with dual band-notched characteristics, AEU - International Journal of Electronics and Communications vol. 128, (2021) pp. 153505.